Radiometric Waveguide Calibrators

E.J. Wollack[1], D.J. Fixsen[2], A. Kogut[1], M. Limon[2], P. Mirel[2], J. Singal[3]

Exploration of the Universe Divsion[1]
NASA Goddard Space Flight Center, Code 665
Greenbelt, MD 20771
email: edward.j.wollack@nasa.gov

[2] Science Systems and Applications, Inc.
NASA Goddard Space Flight Center, Code 665
Greenbelt, MD 20771

[3] Department of Physics, University of California
Broida Hall, Building 572
Santa Barbara, CA 93106

Abstract: We describe the electromagnetic and thermal design, performance, and fabrication for two types of radiometric waveguide load calibrators. A simple theory is presented, and used to minimize the total volume of the absorber structure. These devices have been used from room temperature to below 4 K in microwave to millimeter wavebands. The estimated precision of the calibrator is better than 1 mK absolute at temperatures near 2.7 K.

Introduction: A microwave power standard can be realized by terminating a transmission line with a load of known physical temperature. The absolute exchangeable noise power, $P = k_b T \Delta \upsilon \, x / (e^x - 1)$, where $x = h\upsilon / k_b T$, k_b is Boltzmann's constant, T is the physical temperature of the load, and $\Delta \upsilon$ is the effective RF bandwidth of the received power, can be determined through the measurement of the load's physical temperature. This expression reduces to the Nyquist equation, $P \approx k_b T \Delta \upsilon$, in the Rayleigh-Jeans limit where $x << 1$. The design described here is used as an internal reference load or transfer standard. By accounting for the calibrator mismatch and emission from the interconnecting guide section such structures can be employed as precision absolute power standards [1,2,3]. Descriptions of prior cryogenic waveguide load art can be found in [4-10].

For radiometric calibration it is desirable to minimize the thermal capacity of the absorber structure while maximizing the thermal conductivity of the loading material. This minimizes the errors in the determination of the emitting material's physical and associated brightness temperatures. Commonly used load configurations include absorbing cones, pyramids, and thin vanes mounted in a waveguide. Although these configurations can have very low return loss, the poor thermal contact between the waveguide wall and the bulk of the absorber allows thermal gradients to form which complicate the mapping of a readout thermometer to the brightness temperature. An ideal calibrator load would have no reflection, finite volume, operate in equilibrium with the incident radiation field, and have an isothermal temperature profile. In this limit a single readout thermometer would be sufficient to determine the information required to compute the load power. We describe two configurations which reasonably approximate these properties by achieving a return loss >30dB while possessing thermal gradients less than 1 mK internal to the calibration load. The designs allow placement of the thermal sensor with minimal impact on the electromagnetic performance.

In this paper we describe a class of load configurations which achieve this goal by using high index lossy dielectric wedge shaped absorbers attached to the waveguide walls. See Figure 1a for a schematic description of the load geometries under consideration. Compared to a conical or pyramidal load centered in the waveguide, this choice results in an increase in minimum feature size, improved mechanical reliability, greater thermal coupling between the load and the temperature sensing elements and the thermal reference, and a reduction in the required total calibrator mass. The design depicted in Figure 2, which we refer to as an inverse wedge, is well suited for wavelengths shortward of a millimeter where the primary design consideration is the realization of circuit elements with maximal size (i.e., other elements of the component dominate the total heat capacity) and minimal sensitivity to the detailed geometry of the structure. The design depicted in Figure 3, a compound wedge taper, is amendable to decimeter to centimeter wavelengths where minimal calibrator mass and volume are design drivers.

Electromagnetic Design: Limiting the total absorber volume and thermal gradients within the device is crucial in controlling the systematic errors which can potentially limit knowledge of the effective emission temperature from the calibrator's termination. The attenuation length sets the scale for the thickness of the emitting region. For a lossy material the skin depth in a bulk material is $\delta = \lambda_o \big/ \pi \sqrt{2 \cdot \left(\varepsilon_r'' \mu_r' + \varepsilon_r' \mu_r'' \right)}$, where λ_o is the wavelength in free space and $\varepsilon_r = \varepsilon_r' + i \cdot \varepsilon_r''$ and $\mu_r = \mu_r' + i \cdot \mu_r''$ are the complex relative permittivity and permeability of the absorbing material. For the materials and frequency range under consideration to a good approximation, $\mu_r \approx 1$. Thus, in the high frequency limit, the influence of magnetic loss is small and the skin depth is,

$\delta \sim \lambda_o \big/ \pi \sqrt{2 \cdot \varepsilon_r{}''}$. Maximizing the imaginary amplitude of the dielectric constant in a manner which is compatible with the absorption length will minimize the required absorber thickness and potential thermal gradients, however, layer thicknesses greater than one skin depth are desirable to minimize the influence of the metal waveguide structure beneath the absorber. In applying these ideas to a rectangular waveguide one notes that the cutoff wavelength and the wave impedance are reduced as the fraction of the guide occupied by dielectric is increased [11]. To realize a load with a low reflection as well as high absorption, appropriate attention to the transformation of the modes and impedance in the structure must be observed.

A lossy dielectric mixture with a disordered metallic system was chosen as the conductive loading material [12]. This choice reduces the change in electrical parameters with ambient temperature, allows the dielectric constant properties to be tailored for the application, and offers improved survivability with thermal cycling over commercially available alternatives. For the calibrators described here, a formulation of Stycast 2850 FT [13] loaded with 30% stainless steel [14] by volume is the preferred material. We refer to this mixture as 'steelcast'. This formulation has a relative dielectric constant of $\varepsilon_r = \varepsilon_r{}' + i \cdot \varepsilon_r{}'' \approx 10.7 + 2.4i$ at centimeter to millimeter wavelengths and represents the highest index loading which is suitable for casting with this mixture. By using a smaller stainless steel power volume fraction, other dielectric values can be realized.

The overall length of the absorber structure is determined by the need to have the structure's absorptance large enough so that radiation traversing the length of the structure, reflecting off the back end of the load, and returning, is small compared to the power reflectance of the taper. Roughly speaking, we require that the square of the integrated absorptance to be large compared to the taper's reflectance. If this condition in not achieved, the unabsorbed radiation will increase the overall load reflectance. As the length of the absorber is increased, the absorptance improves, but the tip angle for the absorber becomes increasingly difficult to reliably fabricate. The amplitude reflection coefficient, $\Gamma < \sqrt{A_{tip}} \big/ 2b_o$, of a conical load or pyramidal in a rectangle waveguide of height b_o is governed by the achievable point area , A_{tip} [16]. Thus, in order to produce a low reflectance load of this type, minimizing the tip area is a key design parameter. Realizing small area tips can be challenging, give the mechanical properties of castable absorbers. To achieve reflectivities less than -40dB the details of the flange geometry also needs to be considered.

We can reduce the sensitivity to the absorber insert tip geometry by a factor of ~2 to 4 by moving the tip from the center of the guide to the waveguide corner, where the electric field strength is lower. The absorber is then tapered to follow a compound catercorner to the waveguide crossection. See Figure 3. We call this configuration a compound wedge taper. We find that this geometry results in a more compact load than the single parameter wedge tapers summarized in

Figure 1b which have $\theta_{taper} > 0^o$. In addition, this configuration provides a convenient means to improve the thermal coupling between the portion of the load profile which is responsible for the thermal emission and the thermometer. Alternatively, one could imagine producing an extremely low reflectance termination by using guide with finite conductivity and infinite length. This can be approximated in practice by adiabatically loading a waveguide transition having $\theta_{taper} < 0^o$ with a high index lossy dielectric material. We call this configuration an inverse wedge load. For both configurations we find a layer which is $\Delta \geq 0.7 \cdot b_o > \delta$ in thickness compatible with our thermal goals and has a reflectivity which is reasonably insensitive to the overall geometry.

In general, the absorptance of a waveguide structure is a complicated function of material parameters, geometry, and frequency. More precise physical and analytical insight into the performance of a waveguide termination can be gained by considering the reflection coefficient amplitude, Γ, and by conservation of energy for a one-port device. The response of a lossy adiabatic taper can be estimated from the integral of the differential reflection coefficient [17],

$$
\begin{aligned}
\Gamma &\cong \int_0^L \exp\left(2i \int_0^z \gamma(z') \cdot dz' \right) \cdot d\Gamma \\
&= \int_0^L \exp\left(2i \int_0^z \gamma(z') \cdot dz' \right) \cdot \left\{ \frac{1}{2} \frac{d}{dz}(\ln Z) \right\} \cdot dz
\end{aligned}
\tag{1}
$$

where γ is the propagation constant and Z is the characteristic impedance for the guiding structure. This linearized form of the Riccati equation yields accurate results in the frequency regime where $|\Gamma|^2 << 1$. The direction of propagation is along the z-axis, and the length of the absorber structure is L. The taper geometries are evaluated by numerically solving for the effective propagation wavelength in waveguide from the transverse resonance conditions given the complex dielectric constant of the absorber, and the waveguide and taper cross-section geometry. Selected candidate calibrator configurations were subsequently analyzed for sensitivity to the material parameters and geometry with the Ansoft High Frequency Structure Simulator (HFSS) [18].

In Figure 1a and 1b we present the maximum return loss as a function of taper angle for a set of dielectrics loaded in this manner. For this calculation we assume a fixed length for the absorber equal to eight times the broad wall length, symmetrically loaded dielectric slabs of thickness equal to the guide height, and lossless guide walls. We report the maximum return loss for a $a_o : b_o = 2.000 : 1$ rectangular waveguide over the frequency range, $1.2 < f/f_c < 1.9$, where a_o is the waveguide broadwall dimension, b_o is the guide height, and f_c is the cutoff frequency for the input waveguide guide crossection. In the taper angle range of

~3 to 15 degrees the response is set by the wedge geometry essentially independent of the complex dielectric constant; in the range ~ -3 to -15 degrees the details of the dielectric loading can be used to produced enhanced broadband absorption. For these parameters we simultaneously find low reflectance, minimal sensitivity to the detailed dielectric properties, and a convenient working volume for the load assembly. In the approaches studied we produce an adiabatic transition from TE_{10} rectangular guide to dielectric loaded guide by loading both the upper and lower walls of the guide. These configurations produce relatively high attenuation per unit length and have the added benefit of producing minimal impact on the propagation constant in the region where the structure transitions to metal guide.

Thermal Sensor Location: In order to maximize the coupling between the absorbing material and the temperature sensor we place the sensor in the load. An understanding of where the power is dissipated along the load profile is helpful in understanding where the thermal sensors should be located to best determine the load effective brightness temperature with minimal error over the measurement band. The lower the frequency, the larger the load, the more important this consideration has on the design. This can be explored from the field solutions of the finite element model; however, a more instructive picture is revealed by considering the form of Equation 1. We note that the absorption should scale approximately as the guide wavelength for an adiabatic transition.

The power distribution along the load structure was experimentally derived from a set of 2-port S-parameter measurements where the total absorber length was changed in a controlled manner. For each measurement trail material from the back end of the load was trimmed, the load length measured, and the power absorption was computed from the observed response with the wedge load sample placed in a section of WR28.0 housing. See Figure 4a for the average response of eight trails. The gradient of the power absorption as a function of guide wavelength was computed from the observed data and presented in Figure 4b.

To minimize the error in determination of the load's ambient temperature in the presence of thermal gradients it is desirable to embed the thermal sensor near the position of the peak absorbed power along the length of the absorber. Since the position is approximately fixed in guide wavelengths, in physical length units, the position moves with frequency due to the guide dispersion. Similar considerations indicate that at low frequencies the effective length where the absorption takes place is wider than at high frequencies. The increase in reflectance at the low end of the band typically occurs when the position of the peak power absorption exceeds the length of the taper. In this limit, the adiabatic approximation used to derive the response of the lossy impedance transformer breaks down.

Measured Calibrator Reflectance: We present measured scattering parameters for representative load designs. The Hewlett Packard 8510C Vector Network Analyzer was calibrated with a TRL (Thru-Reflect-Line) calibration. A ~20 cm section of phosphor-bronze guide was employed as a thermal break between the network analyzer and the device under test while at liquid nitrogen temperatures. Reflectance measurements for a typical compound wedge design example are given in Figures 5. In Figure 6, the corresponding data for an inverse wedge load design is presented. Simulated variations in load thickness and dielectric properties are also displayed to convey representative parameter sensitivity.

Thermal Design: A low reflection coefficient alone is not sufficient for a calibration load. The temperature must be determined as well. While an effective temperature could be inferred from a combination of thermometers, the direct approach of making an isothermal calibrator is easier to analyze and easy to reliably realize. In this limit, the time evolution of the device power is

$$P(t) = C \cdot \frac{dT}{dt} + G \cdot \delta T \tag{2}$$

where P is the power delivered to the load, C is its heat capacity, and δT and G are respectively the temperature rise and thermal conductance of the load with respect to a thermal reservoir. For a step function change in power of amplitude P_o, the temperature evolves as,

$$\delta T = \frac{P_o}{G} \cdot (1 - \exp(-t \cdot G/C)) \tag{3}$$

and allows the association of the ratio C/G with the structure's thermal time constant, τ. The thermal configuration employed for the calibrator is shown in Figure 7. In practice, we run the reference calibrator at 2.7 K which is thermal equilibrium with the source radiation with $\tau \sim 10$ seconds. This choice minimizes the potential influences of the heating/cooling the load, losses, and uncertainly in temperature determination.

The load material has a relatively low thermal conductance (κ = 0.02 W/m/K at 2.7 K), but the wedge design allows a short (less than 2 mm) path to the aluminum mounting plate. Aluminum is a inexpensive material with reasonably high thermal conductivity (κ = 23 W/m/K at 2.7 K). This in turn is surrounded by the copper waveguide (κ = 160 W/m/K at 2.7 K). In order to reduce the temperature gradients to less than 1 mK the waveguide is thermally isolated with a section of thin wall (250 μm) stainless steel (κ = 0.15 W/m/K at 2.7 K) waveguide. The thermometer is a RuO thermometer [19] embedded in the steelcast near the region where most of the radiation is emitted/absorbed. The RuO thermometer has approximately 0.1 mK precision and is calibrated to better

than 1 mK absolute accuracy. The sensor's envelope is 1.27 mm x 1.27 mm x 0.44 mm (0.050" x 0.050" x 0.018"). The average power dissipated during readout is 0.6 nW so the thermometer introduces negligible gradients in the temperature.

In order to further reduce thermal gradients the copper waveguide is surrounded by Styrofoam [20] insulation (κ = 0.004 W/m/K at 2.7 K, density ~ 0.025 [gm/cm^3]) and this in turn is encapsulated in a copper can. The heater to maintain thermal control and thermal link to the cryogenic bath are coupled to this copper can rather than the waveguide or aluminum wedge. The waveguide thus acts as a thermal "open circuit" with no steady-state heat flow through the waveguide or the absorber. The copper can is surrounded by a second layer of foam which in turn is surrounded by an aluminum can to provide additional isolation from the environment. Heater power of ~50 mW warms the load 1K above the bath temperature of 1.5K. The maximum thermal gradient that could possibly be maintained at load temperature near 2.7 K is ~4 mK; however, an engineering element model of the assemble suggests that gradients ~0.05 mK are more likely.

One concern is the thermal time constant of the calibrator. A fast time constant allows rapid temperature change, but if it is faster than the thermometer readout it allows the temperature changes to go unmeasured. Therefore a minimum time constant should be the read rate of the thermometer (~1 sec). However, the control loop (PID) becomes easier to optimize if the time constant is a few times the read time. In our application, the time constants were chosen to be ~10 sec. At 2.7 K, the heat capacity of the structure is dominated by the steelcast absorber (κ = 4 J/kg/K at 2.7 K). This assures that there are no sections of the load changing temperature without being measured by the thermometer.

The thermometers (RuO) were calibrated in situ after the loads were completed. To calibrate, the waveguide is bolted directly to an aluminum plate which is temperature controlled via a PID controller. The thermometer for this control is a second RuO thermometer calibrated by NIST which shares the same ohm meter as the load thermometer. The aluminum plate is stood off from the control surface and shielded from the environment so it acts as a thermal "open circuit" with no heat flow through this interface or the waveguide. This plate is weakly coupled to a pumped helium bath which is varied in temperature from 1.4 to 4.2 K. The calibration is repeatable to 1 mK [19].

For an absolute radiometric measurement, one desires to measure the temperature of the active part of the absorber, to the limit of the accuracy of the readout electronics. For the WR112 calibrator, the thermometer size is small with respect to the thickness of the absorber, so placement near the region with maximum thermal emission does not present a fundamental microwave design issue. The general topology described for thermally buffering the calibrator from its environment has been used on all of the calibration assemblies described

here. For the inverse wedge loads, from a thermal perspective, the role played by the aluminum insert and copper waveguide are replaced by the split-block housing. At shorter wavelengths (e.g., WR10.0), we incorporate a relief pocket and small hole thru the split-block which minimize the impact of the thermal sensor and its bias leads on the inverse wedge load's reflectivity. This approach allows flexibility in the placement and encapsulation of the thermal sensor near the region where the dominant portion of the thermal emission occurs. For broadband radiometric applications, the use of redundant sensors is recommended if high precision is required.

Although we have measured and describe the load as used at 2.7K, there is very little that needs to be changed for operation at other temperatures. The RuO thermometer is optimal for 1-10 K but any small thermometer suitable for the temperature range of interest could be substituted for the RuO thermometer. As the temperature increases the heat capacity typically rises faster than the thermal conductivity so the time constant tends to rise with temperature. But as long as the time constants are not too long for the application the same load could be used up to ~350 K. At that temperature the epoxy starts to degrade. The same thermal isolation is useful in a laboratory environment. In the laboratory convection in air can cause unwanted thermal variation. The foam and can arrangement effectively eliminates convection on the outside of the load. Inside the waveguide, convection can be eliminated by pointing the input down while heating the load. This leaves the gas stratified (i.e., warmer gas above the cooler gas). Of course, if the load were operated cooler than the environment, it should be pointed up.

The integration of the metal backing plate with the absorber material reduces thermal gradients in the structure and thereby improves the experimental accuracy to which the power emitted by the load is known. We note for high power applications this improvement in thermal conductivity could also improve the power handing capabilities of the load. From a tolerance perspective, a compound wedge load is difficult to conveniently fabricate for wavelengths shorter than ~2 cm. Since the inverse wedge load is directly cast in the waveguide housing the relatively thin portion of the load is supported throughout its manufacture. This enables fabrication down to a scale limited by the viscosity of the uncured loaded dielectric mixture. For the 30% steelcast mixture we employ, the minimum thickness is ~100 μm, suggesting this approach could find potential applications down to submillimeter wavelengths.

ACKNOWLEDGMENT:

REFERENCES:

[1] C.K.S. Miller, W.C. Daywitt, and M.G. Arthur, "Noise Standards, Measurements and Receive Noise Definitions," 1967, Proceedings of the IEEE, Vol. 55, No. 6, pp. 865-877.

[2] F.-I. Buchholz and W. Kessel, "A New Primary Thermal Noise Standard at PTB for the Frequency Range of 12.4-18.0GHz," 1993, IEEE Transactions on Instrumentation and Measurement, Vol. 43, No. 2, pp. 258-263.

[2] J. Achkar, "A Set of Waveguide Primary Thermal Noise Standards and Related Calibration Systems for the Frequency Range of 8.2-40GHz," 1999, IEEE Transactions on Instrumentation and Measurement, Vol. 48, No. 22, pp. 638-641.

[3] B. Vowinkel, "Broad-band Calorimeter for Precision Measurement of Millimeter- and Submillimeter-Wave Power," 1980, IEEE Transactions on Instrumentation and Measurement, Vol. 29, No. 3, pp. 183-189.

[4] C.T. Stelzried, "Microwave Thermal Noise Standards," 1968, IEEE Transactions on Microwave Theory and Techniques, Vol. 16, No. 9, pp. 646-655.

[5] T. Mukaihata, "Applications and Analysis of Noise Generation in N-Cascaded Mismatched Two-Port Networks," 1968, IEEE Transactions on Microwave Theory and Techniques, Vol. 16, No. 9, pp. 699-708.

[6] A.A. Penzias, "Helium Cooled Reference Noise Source in a 4kMc Waveguide," 1965, Review of Scientific Instruments, Vol. 36, pp. 68-70.

[7] C.L. Trembath, D.F. Wait, G.F. Engen, W.J. Foote, "A Low Temperature Microwave Noise Standard," 1968, IEEE Transactions on Microwave Theory and Techniques, Vol. 16, No. 9, pp. 709-741.

[8] L. R. D'Addario, "An SIS Mixer for 90-120 GHz with Gain and Wide Bandwidth," 1984, International Journal of Infrared and Millimeter Waves, Vol. 5, No. 11, pp. 1419-1444.

[9] W.R. McGrath, A.V. Raisanen, and P.L. Richards, "Variable Temperature Loads for Use in Accurate Noise Measurements of Cryogenically-Cooled Microwave Amplifiers and Mixer," 1986, International Journal of Infrared and Millimeter Waves, Vol. 7, No. 4, pp. 543-553.

[10] A. R. Kerr, H Moseley, E. Wollack, W. Grammer, G. Reiland, R. Henry, K.P. Stewart, "MF-112 and MF-116: Compact Waveguide Loads and FTS Measurements at Room Temperature and 5 K," 2004, ALMA Memo 494. http://www.alma.nrao.edu/memos/

[11] N. Marcuvitz, *Waveguide Handbook,* 1951, MIT Radiation Laboratory Series, McGraw-Hill, New York, Vol. 10, pp.16-24, 391-393.

[12] Wollack, E.J., Fixsen, D.J., Ross, H., Kogut, A., Limon, M., Mirel, P, "Electromagnetic Properties of a Conductively Loaded Epoxy," 2006, submitted.

[13] Emerson & Cuming, "Stycast 2850 FT Two Component, Versatile Epoxy Encapsulant with High Thermal Conductivity," Technical Data Sheet, E290/09/99-RVH/MVR

[14] Micro-Melt 316L, 16 micron diameter stainless steel power; Carpenter Power Products Inc., 600 Mayer Street, Bridgeville, PA 75017

[15] Eccosorb Lossy, Magnetically Loaded Castable Resin (CR) Machinable Stock (MF) Absorbers, Emerson & Cuming Microwave Products, Randolph, MA 02368, http://www.eccosorb.com

[16] W.B.W. Alison, "A Handbook for the Mechanical Tolerancing of Waveguide Components," 1987, Artech House, MA, pp. 346-368.

[17] R.E. Collin, "Foundations for Microwave Engineering", Second Edition, 1992, McGraw-Hill, New York, pp. 383-386.

[18] Ansoft, HFSS (High Frequency Structure Simulator), 225 West Station Square Drive Suite 200, Pittsburgh, PA 15219.

[19] D.J. Fixsen, P.G.A. Mirel, A. Kogut, M. Seiffert, "A Low Noise Thermometer Readout for Ruthenium Oxide Resistors," 2002, Review of Scientific Instruments, Vol. 73, No. 10, pp. 3659-3663.

[20] Dow-Chemical, Styrofoam Scoreboard Brand Extruded Insulation, Midland Michigan.

Figure Captions:

Figure 1a and 1b: Wedge Load Response as a Function Taper Angle. The upper panel depicts several E-plane load crossections for selected taper angles. In all of the dielectric absorber models considered the material thickness is limited to a constant thickness, Δ, as shown. A taper angle of +90 degrees corresponds to reflection off dielectric plug filling rectangular waveguide section for the dielectrics loadings considered, 0 degrees is an interface between lossless guide and infinite guide with finite loss, and -90 degrees is an abrupt change in guide height where the symmetric steps are filled with lossy dielectric. The lower panel shows the maximum return loss for an absorber thickness $\Delta = 0.7 b_o$ over the frequency range $1.2 < f/f_c < 1.9$. The parameters chosen for the simulations in the lower panel are representative of achievable dielectric loadings. The filled symbols are the calculations and a line has been added to guide the eye. The four open diamonds with error bars are the measured data for examples of loads we have fabricated and tested.

Figure 2: Rectangular Waveguide Inverse Wedge Load Cross-section (WR28.0 Waveguide; Cutoff Frequency, f_c = 21.07 GHz). The upper and lower wedge load sections were cast in the waveguide split-block. For clarity, one half of the split-block is not displayed. A piece of Teflon with the shape of the waveguide interior was used as a form during the molding process to define the -3.0 degree wedge descent angle. A 0.010" (0.25mm) stainless steel waveguide section, length 1.75" (44.4mm), is used to thermally decouple the load from other elements of the test apparatus.

Figure 3: Rectangular Waveguide Compound Wedge Load (WR112 Waveguide; Cutoff Frequency, f_c = 5.263 GHz). The lossy dielectric absorber layer is cast on a metal insert which in turn is attached to the waveguide wall (i.e., the absorber material is aligned catercorner in the guide). The taper accent angles are +10.0 and +19.1 degrees with respect to the waveguide short and broad-walls. A 0.010" (0.25 mm) stainless steel waveguide section, length 3.25" (82.6 mm), is used to thermally decouple the load from other elements of the precision radiometer.

Figure 4a and 4b: Measured Power Absorption for a $\theta_{taper} \cong +10^o$ Wedge Load. Distance from load to tip is measured in units of guide wavelengths, $\lambda_g \equiv \lambda_o / \sqrt{1 - (\lambda_o / \lambda_c)^2}$, for the input waveguide crossection. Here λ_o and $\lambda_c = 2a_o$ are respectively the free-space and input guide section's cutoff wavelength. The data in the lower panel has been normalized to unity at absorption gradient peak for clarity of presentation. The symbol size was chosen to be representative of

the uncertainties arising from the sample geometry and the observed measurement repeatability.

Figure 5: Measured and Modeled Power Reflection from WR112 Compound Wedge Load (Waveguide Cutoff Frequency, f_c = 5.263 GHz). The squares indicate the modeled response for a lossy dielectric absorber thickness greater than or equal to 70% of the guide height. As indicated by the diamonds, the absorption degrades as the absorber thickness is reduced due to the incident wave interacting with the metal backing layer. The solid red and dashed blue lines are the measured response at 296K and 77K respectively. The observed slight change in response in cooling is repeatable and largely due to the change in the calibrator's dimensions.

Figure 6: Measured and Modeled Reflected Power from WR28.0 Inverse Wedge Load (Waveguide Cutoff Frequency, f_c = 21.07 GHz). Two differing dielectric loadings, representative of 30% steelcast (solid blue line) and CR112 (solid red line) [15], are presented. The finite element model for CR112 with $\varepsilon_r = 3.9 + 0.5i$ is denoted by circles in the figure. One observes by increasing the dielectric constant magnitude the low frequency response is improved.

Figure 7: Cryogenic Calibrator Assembly Crossection and Thermal Detail.
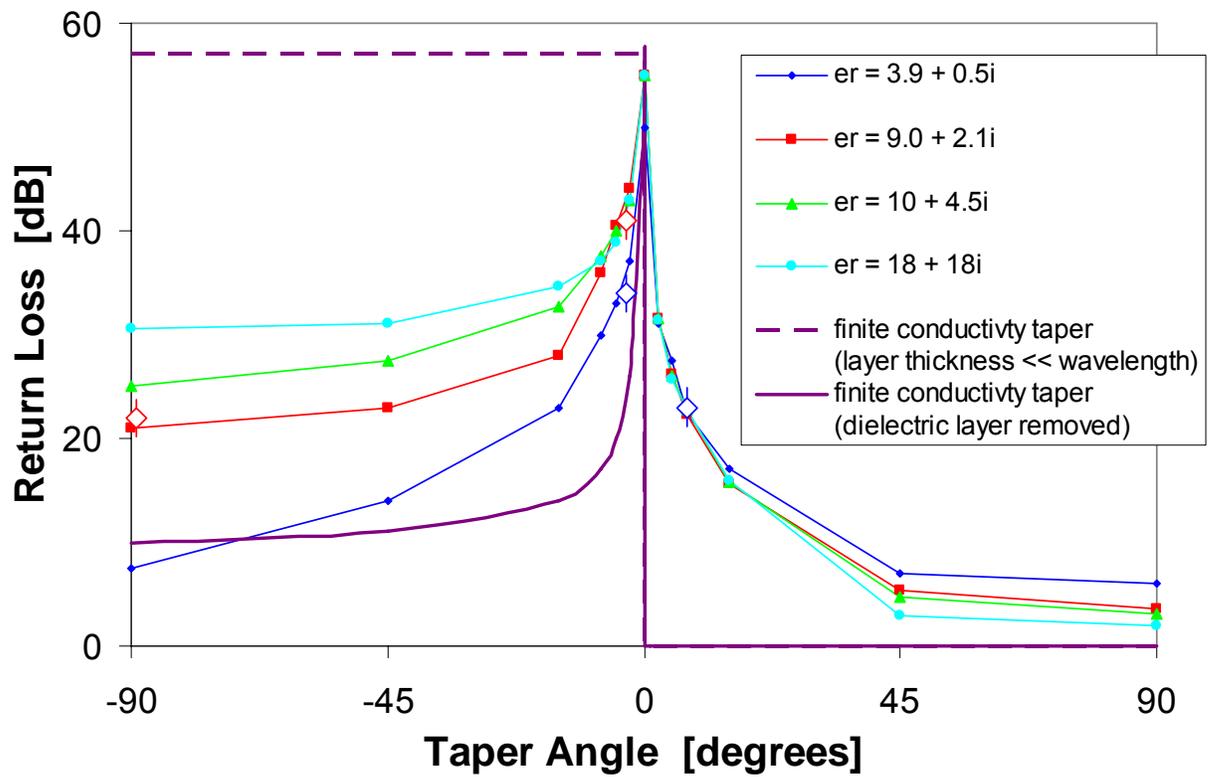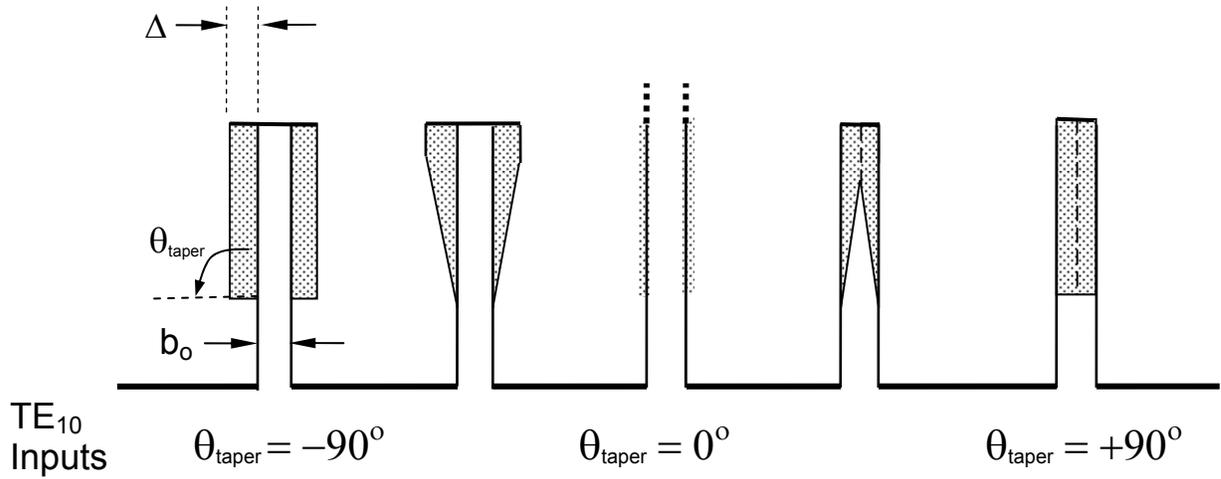
Figure 1a and 1b: Wedge Load Response as a Function Taper Angle.
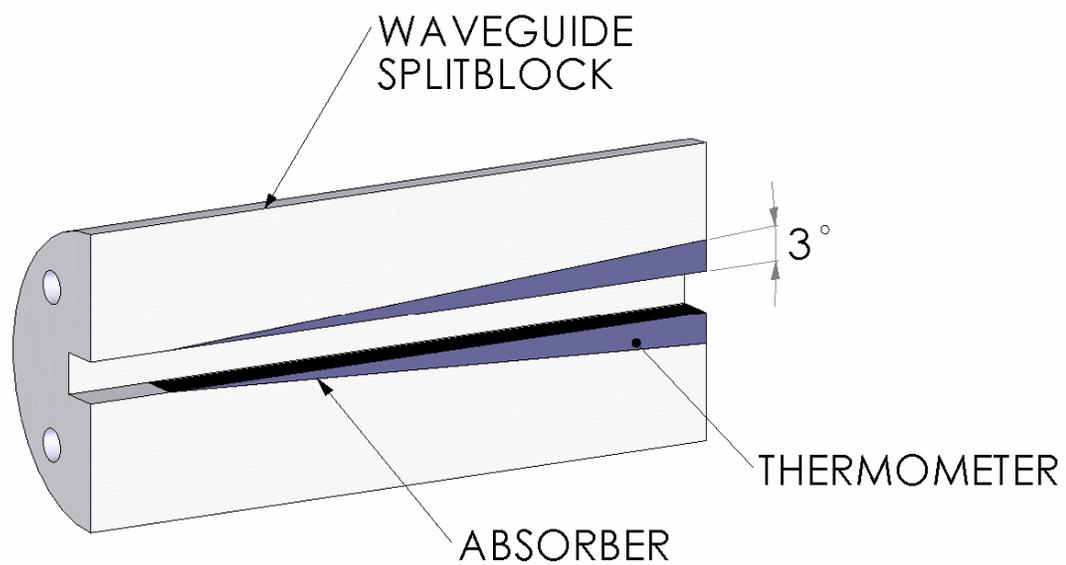
Figure 2: Rectangular Waveguide Inverse Wedge Load Cross-section (WR28.0 Waveguide; Cutoff Frequency, f_c = 21.07 GHz).
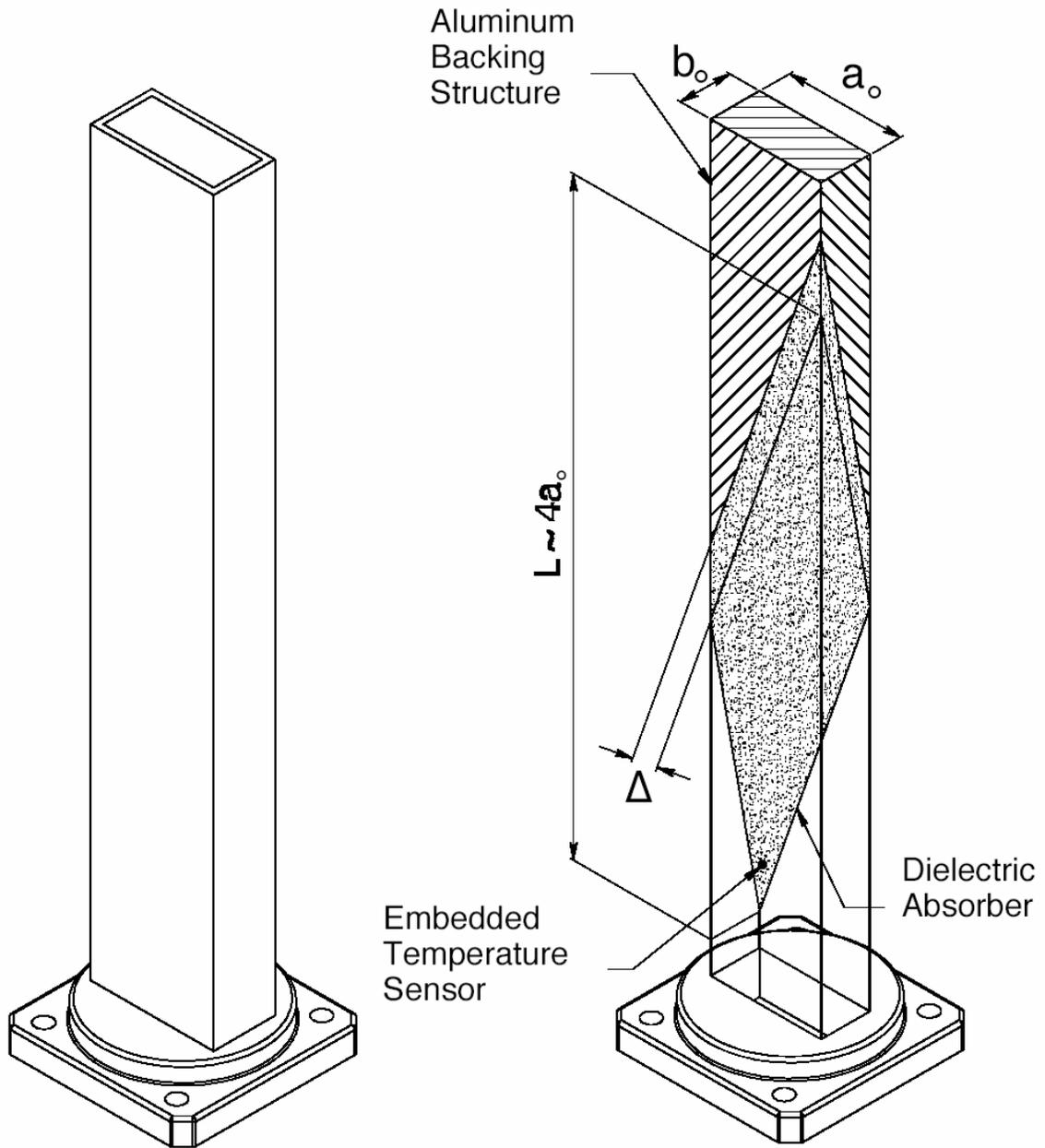
Figure 3: Rectangular Waveguide Compound Wedge Load (WR112 Waveguide; Cutoff Frequency, f_c = 5.263 GHz).
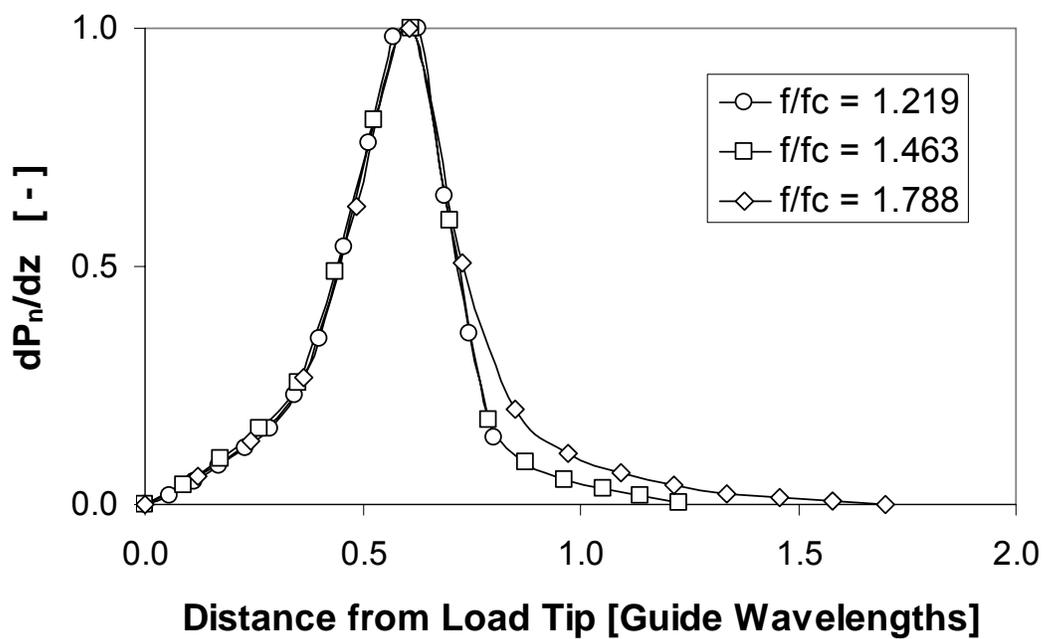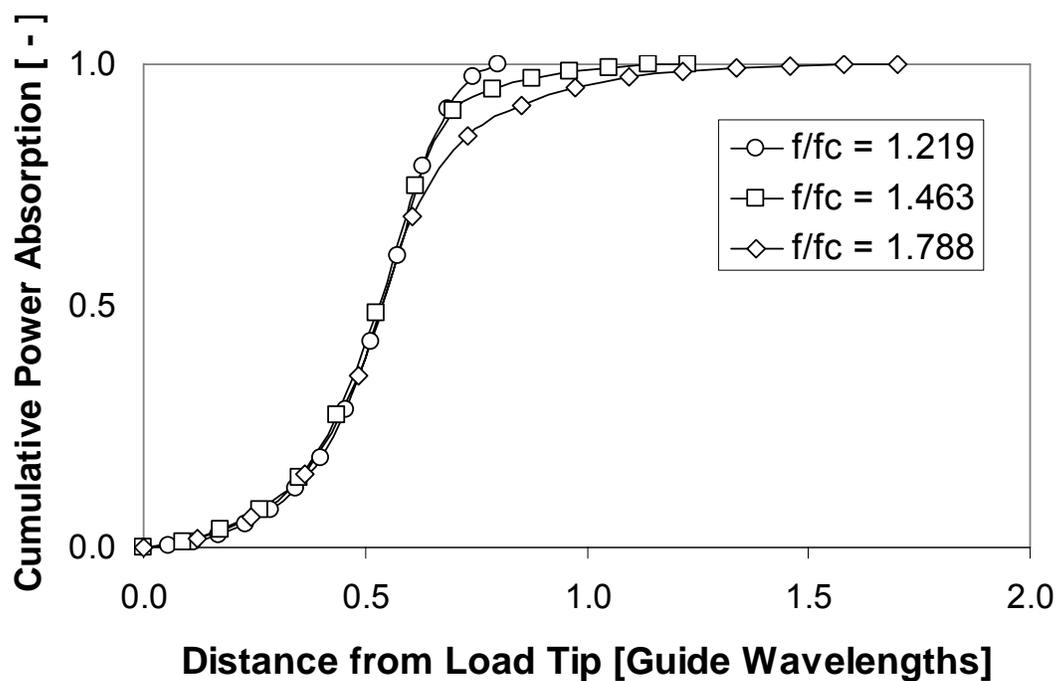
Figure 4a and 4b: Measured Power Absorption for a $\theta_{taper} \cong +10^{o}$ **Wedge Load.**
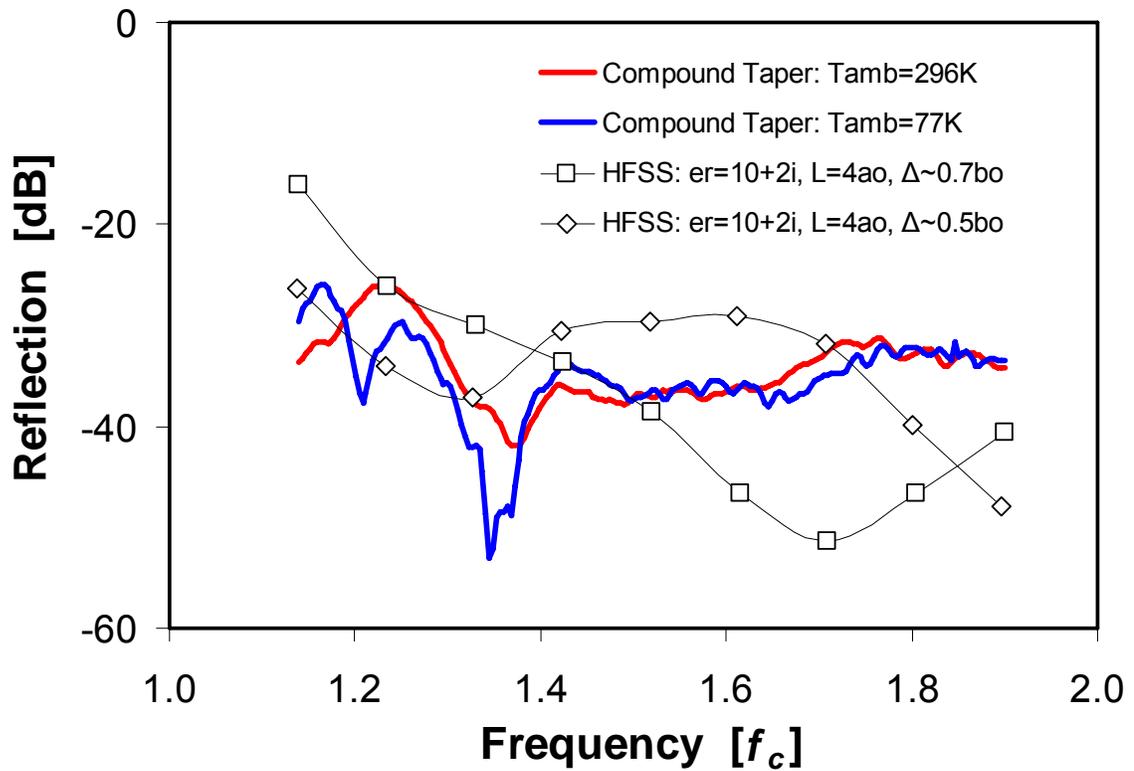
Figure 5: Measured and Modeled Power Reflection from WR112 Compound Wedge Load (Waveguide Cutoff Frequency, f_c = 5.263 GHz).
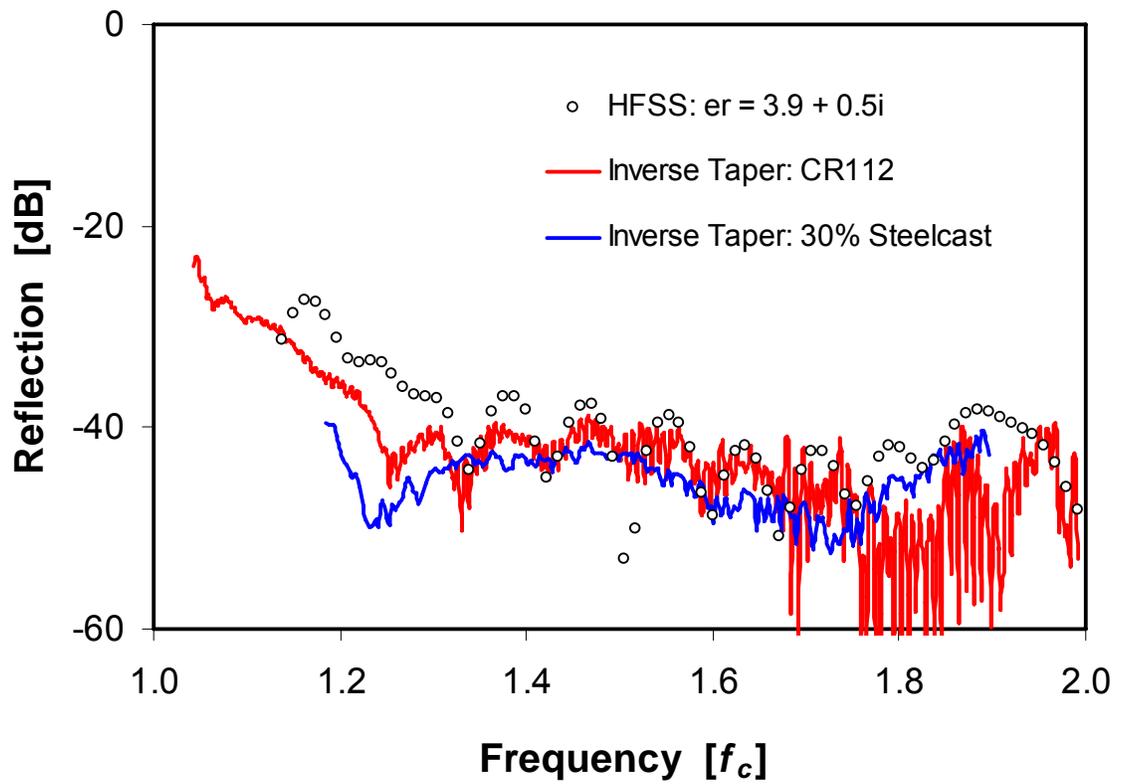
Figure 6: Measured and Modeled Reflected Power from WR28.0 Inverse Wedge Load (Waveguide Cutoff Frequency, f_c = 21.07 GHz).

Figure 7: Cryogenic Calibrator Assembly Crossection and Thermal Detail.